Laminin is required for Schwann cell morphogenesis

Wei-Ming Yu[1], Zu-Lin Chen[1,*], Alison J. North[2] and Sidney Strickland[1,*]

[1]Laboratory of Neurobiology and Genetics, The Rockefeller University, New York, NY 10065, USA
[2]Bio-Imaging Resource Center, The Rockefeller University, New York, NY 10065, USA
*Authors for correspondence (e-mails: chenz@mail.rockefeller.edu; strickland@mail.rockefeller.edu)

Accepted 24 November 2008
Journal of Cell Science 122, 929-936 Published by The Company of Biologists 2009
doi:10.1242/jcs.033928

Summary

Development of the peripheral nervous system requires radial axonal sorting by Schwann cells (SCs). To accomplish sorting, SCs must both proliferate and undergo morphogenetic changes such as process extension. Signaling studies reveal pathways that control either proliferation or morphogenesis, and laminin is essential for SC proliferation. However, it is not clear whether laminin is also required for SC morphogenesis. By using a novel time-lapse live-cell-imaging technique, we demonstrated that laminins are required for SCs to form a bipolar shape as well as for process extension. These morphological deficits are accompanied by alterations in signaling pathways. Phosphorylation of Schwannomin at serine 518 and activation of Rho GTPase Cdc42 and Rac1 were all significantly decreased in SCs lacking laminins. Inhibiting Rac1 and/or Cdc42 activities in cultured SCs attenuated laminin-induced myelination, whereas forced activation of Rac1 and/or Cdc42 in vivo improved sorting and hypomyelinating phenotypes in SCs lacking laminins. These findings indicate that laminins play a pivotal role in regulating SC cytoskeletal signaling. Coupled with previous results demonstrating that laminin is critical for SC proliferation, this work identifies laminin signaling as a central regulator coordinating the processes of proliferation and morphogenesis in radial axonal sorting.

Supplementary material available online at
http://jcs.biologists.org/cgi/content/full/122/7/929/DC1

Key words: Schwann cell, Myelin, Laminin, Morphogenesis, Cytoskeleton

Introduction

Myelination of peripheral nerves is accomplished by Schwann cells (SCs). SCs, derived from the neural crest, differentiate into myelinating or non-myelinating cells. SCs destined to myelinate will proliferate, extend cytoplasmic processes into axon bundles, separate them into smaller bundles, and establish a one-to-one relationship with individual large axons. This process is known as radial axonal sorting (Jessen and Mirsky, 2005).

Radial sorting of axons is accomplished by several distinct but concerted steps: SC proliferation, establishment of spindle shape, and process extension (Martin and Webster, 1973). SC proliferation is essential for the establishment of a one-to-one ratio of myelinating SCs and axons, whereas bipolar shape formation followed by process extension on the radial axis is required for interdigitation and ensheathment of axons. Axonal neuregulins (NRG1) and laminin signaling are crucial for regulating these steps. NRG1 triggers SC proliferation during development through ErbB receptors (Morrissey et al., 1995; Riethmacher et al., 1997; Salzer et al., 1980). SCs lacking β1 integrin, a laminin receptor, proliferate normally but still show impaired axonal sorting (Feltri et al., 2002).

Two Rho GTPase members, Rac1 and Cdc42, play distinct roles in axonal sorting (Benninger et al., 2007; Nodari et al., 2007). Rac1 acts downstream of β1-integrin activation and is essential for SC process extension and stabilization. Cdc42 can be activated by NRG1 and is required for SC proliferation. These results suggest that SC proliferation and process extension are regulated by at least two distinct pathways: one mediated through ErbB receptors and the other dependent on β1-integrin signaling.

SCs lacking the laminin γ1 subunit lose all laminin expression and show severe impairment of axonal sorting (Yu et al., 2005; Yu et al., 2007). Additionally, SCs lacking laminins exhibit severe reduction in proliferation and decreased ErbB phosphorylation (Yang et al., 2005; Yu et al., 2005). The impairment of radial sorting in laminin-deficient nerves could result from decreased SC proliferation, raising the issue of whether laminins also regulate process extension mediated by β1 integrin. To address this issue, time-lapse live-cell imaging was performed in mouse neuronal co-cultures of SC and dorsal root ganglion (DRG) lacking laminins. We found that laminins are required for SC bipolar morphology formation and process extension. Furthermore, both activated Rac1 and Cdc42 are greatly diminished in laminin-deficient SCs. Treatment with constitutively active Rac1 and/or Cdc42 improves sorting and hypomyelinating phenotypes in SCs lacking laminins. These results demonstrate that laminins coordinate both the ErbB-Cdc42 and β1-integrin–Rac1 signaling pathways to regulate multiple processes during radial axonal sorting.

Results

Establishment of mouse SC-DRG neuronal co-cultures

Mouse SC-DRG co-cultures were used to investigate whether laminins regulate extension of SC processes (Cosgaya et al., 2002; Kleitman et al., 1999). The ensheathment and myelination in this system are induced by addition of ascorbate to stimulate basal lamina deposition. After 8 days in feed that promotes myelination (maintenance media with ascorbate; MF), co-cultures from *P$_0$/Cre:fLAMγ1* mice (Chen and Strickland, 2003; Yu et al., 2005) showed decreased laminin expression in neurite regions and a dramatic reduction of myelination when compared with controls (supplementary material Fig. S1B,C). However, these mutant co-cultures contained an unrecombined *laminin γ1* gene present in neurons and fibroblasts (supplementary material Fig. S1A). The neuronal soma expressed high levels of laminins (arrows in supplementary material Fig. S1C,D), and these non-SC laminins progressively rescued the dysmyelinating phenotype when the co-

Journal of Cell Science

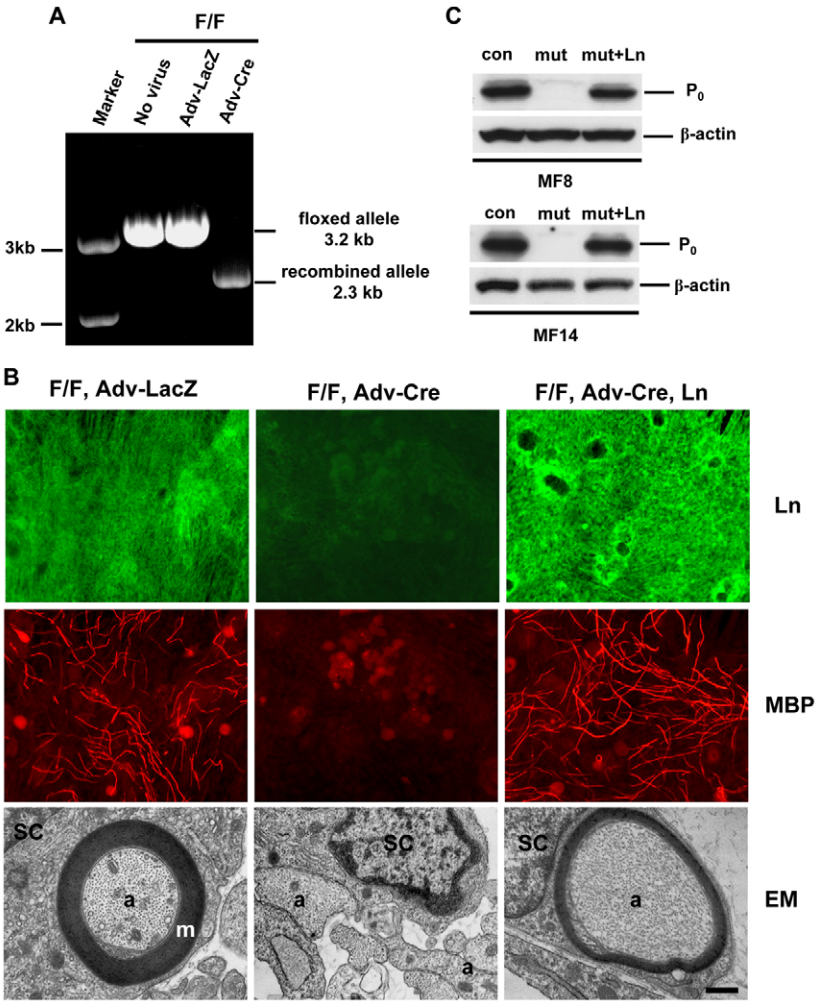

Fig. 1. SCs lacking laminins do not ensheath or myelinate axons. (A) PCR analysis of genomic DNA of co-cultures from homozygous *fLAM γ1* mice (F/F) infected with adenoviruses (Adv) expressing LacZ or Cre. The primers amplified the unrecombined (3.2 kb) and recombined (2.3 kb) *fLAM γ1* alleles. (B) Myelination of mouse SC-DRG co-cultures infected with Ad-LacZ or Ad-Cre 8 days after addition of ascorbate or exogenous laminins was detected by immunostaining for laminins (Ln; green) and MBP (red) or by electron microscopy (EM). Scale bar: 50 μm in Ln/MBP, 1 μm in EM. (C) The expression of myelin protein zero (P0) in co-cultures 8 days (MF8) or 14 days (MF14) after addition of ascorbate was assessed by immunoblotting. β-Actin served as the loading control (con, control; mut, mutant; mut+Ln, mutant with laminins).

cultures were incubated in MF for a longer period (supplementary material Fig. S1D). To circumvent this problem, co-cultures from *fLAMγ1* mice were infected with an adenovirus expressing Cre recombinase (Ad-Cre) to completely disrupt *laminin γ1* (Fig. 1A). In co-cultures infected with a control adenovirus (Ad-LacZ), laminins were present (Ln in Fig. 1B), and myelination was detected 2 days after ascorbate addition. Extensive myelinated fibers were observed after 8 days in MF, and ultrastructural analysis showed normal ensheathment of axons (Fig. 1B). By contrast, laminins were completely absent from Ad-Cre-infected co-cultures, which did not myelinate even after 2 weeks of ascorbate exposure (Fig. 1B,C). Ultrastructural analysis revealed that mutant SCs neither interdigitated between axonal bundles nor properly ensheathed axons (Fig. 1B). Addition of exogenous laminins to the mutant co-cultures restored myelination as well as the defect of ensheathment (Fig. 1B).

SCs lacking laminins do not form bipolar morphology

Bipolar shape formation is the first step of SC differentiation, as SCs must spread radially to a great extent in order to sort and myelinate axons. To determine whether SC morphology was altered upon laminin deficiency, SCs were identified using anti-S100 antibody, myelin sheaths were detected with anti-MBP antibody, and SC morphology upon myelination was visualized using confocal microscopy. After 8 days in MF, most SCs in control co-cultures formed a bipolar morphology and a myelin segment (Fig. 2A). By contrast, SCs lacking laminins did not myelinate and failed to form a bipolar shape (Fig. 2B). Addition of exogenous laminins in mutant co-cultures restored the bipolar morphology and restored myelination (Fig. 2C). Statistical analysis revealed that the length of mutant SCs was significantly decreased as compared with controls (Fig. 2D).

To monitor the real-time morphogenesis of SCs, time-lapse live-cell imaging was performed in co-cultures. To label neurites by red fluorescence and SCs by green fluorescence, co-cultures were infected with two different recombinant adenoviruses at different time points. At the time of plating, the dissociated explants contained mostly neurons and only a few satellite SCs. Cultures were infected with adenovirus expressing mCherry-tagged neurofilament light chain (NFL). Red fluorescence appeared in the soma and proximal neurites within 1 day of infection. By the eighth day, the labeling had extended into the distal neurites (supplementary material Fig. S2A). Two days before imaging (10 days after plating), co-cultures were completely packed with endogenous SCs and were infected with another adenovirus expressing eGFP-tagged β-actin. These eGFP-expressing cells were confirmed as SCs by S100 immunohistochemistry (supplementary material Fig. S2B). The double infection resulted in co-cultures with red axons and green SCs. Infecting co-cultures with these adenoviruses did not impede SC differentiation or myelination (supplementary material Fig.

Journal of Cell Science

Journal of Cell Science

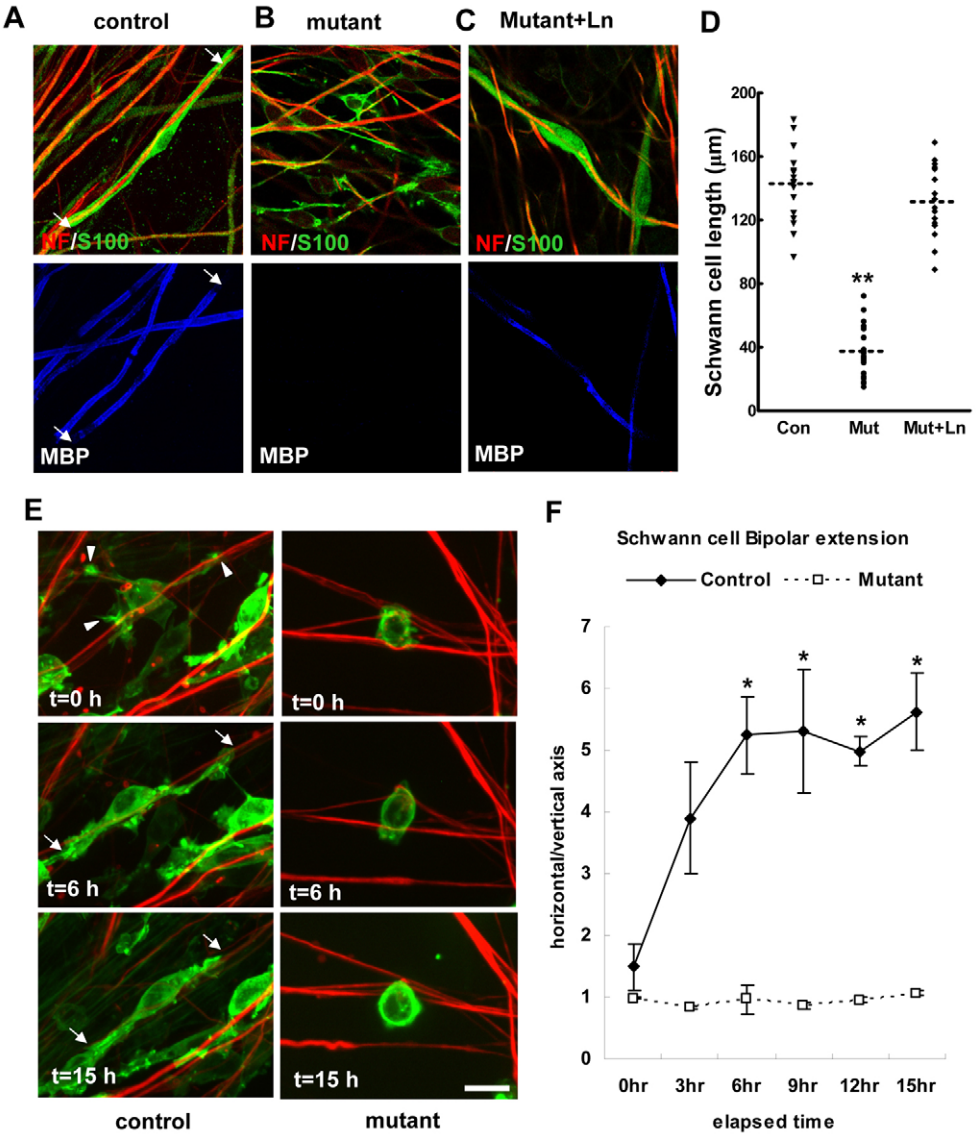

Fig. 2. SCs lacking laminins fail to establish a bipolar morphology. Control (A), mutant (B), and mutant co-cultures with exogenous laminins (C) at MF8 were stained for neurofilment (NF) (red), S100 (green), and MBP (blue). Confocal microscopy was used, and the collected images were merged. (D) Comparison of SC length (measured by S100 staining) in co-cultures at MF8 (three fields per co-culture; six co-cultures in control and mutant+Ln; eight co-cultures in mutant; $^{**}P<0.001$ compared with control). Broken lines represent the average. (E,F) Real-time analysis of the bipolar morphology of SCs. (E) Co-cultures were labeled with Ad-mCherry-NFL and Ad-eGFP-actin and imaged for 16 hours using a spinning disk confocal microscope. Five z-stacks were taken every 15 minutes. Each panel is a maximum projection of the z-stacks. (F) Quantification of the axial axis (parallel to axons) to radial axis (vertical to axons) ratio over a 15-hour period reveals that mutant SCs do not establish a bipolar morphology (duplicate assay; $^{*}P<0.05$; error bars, s.e.m.). Scale bar: 20 μm in A-C, 17 μm in E.

S2C). Labeled co-cultures were imaged for 16 hours with a spinning disk confocal microscope.

This novel approach allowed us to perform high-resolution 3D live-cell imaging to examine the cytoskeletal dynamics of SCs interacting with axons during initiation of myelination. Control SCs established a characteristic bipolar phenotype during initial differentiation (arrows in Fig. 2E; supplementary material Movie 1), as judged by the increasing ratio of the axial axis (parallel to axons) to the radial axis (vertical to axons) over time (Fig. 2F), whereas mutants failed to form a bipolar shape (Fig. 2E; supplementary material Movie 2).

Mutant SCs show less process extension at the onset of myelination

β1-integrin-null SCs proliferate normally but cannot extend radial processes (Nodari et al., 2007). In contrast to β1-integrin mutants, SCs lacking laminins show severe reduction in proliferation. The defects in axonal sorting were thought to be caused by decreased proliferation. However, SCs lacking laminins did not interdigitate between axonal bundles (Fig. 1B), suggesting that laminins might also regulate process extension during sorting. To visualize SC process extension during myelination, time-lapse live-cell imaging with more z-stacks was performed in co-cultures. Imaging of control co-cultures showed that SCs form extensive cytoplasmic processes to attach to neurites (arrows in Fig. 3A; supplementary material Movie 3) and to separate neurites from each other. By contrast, mutant SCs showed less process extension (Fig. 3A; supplementary material Movie 4), and these processes did not attach to neurites. The process extension rate and the length of processes were significantly decreased in mutant SCs (Fig. 3B,C). This result explains why laminin-γ1-mutant mice show the most severe phenotype among all mutants that exhibit defects in radial axonal sorting (Yu et al., 2005; Yu et al., 2007), as disruption of laminins affects both SC process extension and proliferation.

Mutant SCs have impaired cytoskeletal signaling

Mutations in the Neurofibromatosis type 2 tumor suppressor gene, which encodes Schwannomin (merlin), causes schwannomas (Rouleau et al., 1993; Trofatter et al., 1993). Phosphorylation of Schwannomin at serine 518 (Ser518) modifies actin polymerization

Journal of Cell Science

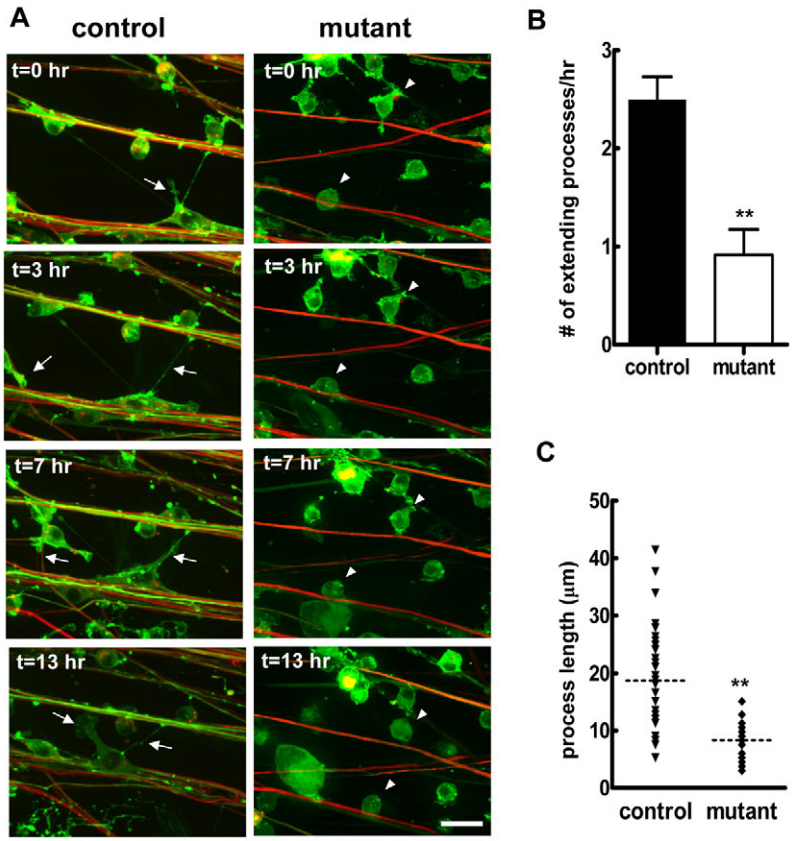

Fig. 3. SCs lacking laminins show decreased process extension. (A) SC-DRG co-cultures were labeled with Ad-mCherry-NFL and Ad-eGFP-actin and then imaged for 16 hours using a spinning disk confocal microscope. Ten z-stacks were taken every 5 minutes. Control SCs show extensive process extension (arrows), whereas mutants form fewer and shorter processes (arrowheads). Scale bar: 20 μm. (B,C) Quantification of process extension rate (B) and the length of processes (C) over a 12-hour period reveals that mutant SCs extend fewer (**P<0.001; error bars, s.e.m.) and shorter (**P<0.001; broken lines represent the average) processes.

and regulates SC morphology (Thaxton et al., 2007a). To investigate whether laminins regulate Schwannomin phosphorylation, total lysates from co-cultures and sciatic nerves were immunoblotted for phospho-Ser518-Schwannomin and total Schwannomin (Fig. 4A). Normalization of phospho-Ser518-Schwannomin to total Schwannomin revealed that the level of phospho-Ser518 was significantly decreased in co-cultures and in nerves lacking laminins (Fig. 4A,B), suggesting that Schwannomin signals were impaired in SCs lacking laminins.

Two Rho GTPase members, Rac1 and Cdc42, regulate podia formation at the cell periphery and are involved in axonal sorting (Benninger et al., 2007; Nobes and Hall, 1995; Nodari et al., 2007). Cdc42 is activated by NRG1-ErbB and is required for SC proliferation, whereas Rac1 is activated by β1 integrin and regulates process extension. SCs lacking laminins have defects in both proliferation and process extension, which led us to examine whether laminins could regulate both pathways to promote axonal sorting. Activated Rac1 and Cdc42 were assessed by affinity precipitation and immunoblot assay using PAK-1 PBD agarose. Activated Rac1 and Cdc42 were significantly increased during the initiation of myelination in control but not in mutant co-cultures and nerves (Fig. 4C,D). Exposure of mutant co-cultures to exogenous laminins partially restored the levels of activated Rac1 and Cdc42 (Fig. 4C,D). It has been shown that Cdc42 is activated by NRG1-ErbB signaling to promote SC proliferation during sorting (Grove et al., 2007). In peripheral nerves lacking laminin in their SCs, phosphorylation of ErbB receptors is decreased (Yu et al., 2005). To further confirm whether phosphorylation of ErbB is decreased in co-culture upon disruption of laminins, total lysates from co-cultures were immunoblotted for phospho-ErbB2 and total ErbB2 (Fig. 5). Normalization of phospho-ErbB2 to total ErbB2 revealed that the level of phospho-ErbB2 was significantly decreased in co-cultures lacking laminins. However, the extent of decrease is not as dramatic as in vivo (Yu et al., 2005), probably because co-cultures contain ErbB proteins from other cell types (i.e. neurons). These results indicate that laminins regulate both ErbB-Cdc42 and β1-integrin–Rac1 signaling pathways.

Inhibition of small GTPase activities attenuates laminin-induced myelination

To test whether laminin-induced myelination in co-cultures depended on Rac1 and/or Cdc42 activities, we modulated Rac1 and/or Cdc42 activities upon onset of myelination by infecting co-cultures with adenoviruses expressing dominant negative or constitutively active Rac1 or Cdc42 (Ad-Rac1DN, Ad-Cdc42DN, Ad-Rac1CA, Ad-Cdc42CA). In mutant co-cultures with exogenous laminins, expression of Cdc42DN or Rac1DN partially attenuated laminin-induced myelination in mutant co-cultures (compare Fig. 6B,C to 6A; quantification in Fig. 6G,I). The amount of inhibition was similar with both Rac1DN and Cdc42DN, indicating that both pathways contribute significantly to myelination. Expression of both Rac1DN and Cdc42DN in mutant co-cultures with exogenous laminins dramatically suppressed laminin-induced myelination (compare Fig. 6D to 6A; quantification in Fig. 6G and 6I). These results agree with previous observations that mice with SC-specific ablation of Rac1 or Cdc42 show hypomyelinated nerves (Benninger et al., 2007; Nodari et al., 2007).

To explore whether increasing Rac1 and/or Cdc42 activities is sufficient to restore myelination in mutant co-cultures, we infected co-cultures with Rac1CA and/or Cdc42CA. We did not observe

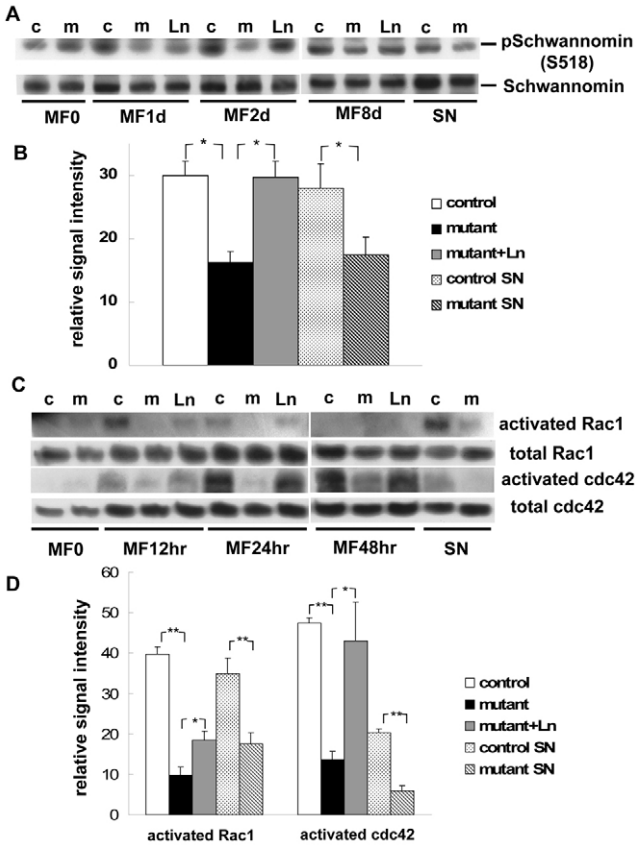

Fig. 4. SCs lacking laminins show aberrant cytoskeletal signaling. (A) Phosphorylation of Schwannomin at Ser518 in control (c), mutant (m), and mutant co-cultures with exogenous laminins (Ln) incubated for 1, 2 and 8 days in MF (MF1d, 2d and 8d, respectively) and in control and mutant sciatic nerves (SN) at postnatal day zero (P0) was assessed by immunoblot. (B) Quantitative analysis of phospho-Ser518 Schwannomin normalized with total Schwannomin level in co-cultures at MF2d and sciatic nerves. Triplicate assays; *P<0.05; error bars, s.e.m. (C) Activated Rac1 or Cdc42 of control (c), mutant (m), and mutant co-cultures with exogenous laminins (Ln) incubated for 12, 24 and 48 hours in MF (MF12hr, 24hr and 48hr, respectively) and in control and mutant sciatic nerves (SN) at P0 was assessed by affinity precipitation-immunoblot assay using PAK-1 PBD agarose. Total cell lysates were fractionated and probed with Rac1-Cdc42 antibody to detect total Rac1 and total Cdc42. (D) Quantitative analysis of affinity precipitation-immunoblot assay of co-cultures at MF12hr (for activated Rac1) or MF24hr (for activated Cdc42) and sciatic nerves shows that activated Rac1 and Cdc42 were both significantly higher in controls than in mutants. Addition of exogenous laminins to mutant co-cultures partially restored the levels of activated Rac1 and Cdc42. Signal intensity of activated Rac1 and Cdc42 (GTP-bound Rac1 and Cdc42) was measured by ImageJ and normalized to total Rac1 or total Cdc42 at the indicated time points. Triplicate assays; *P<0.05, **P<0.01; error bars, s.e.m.

myelin restoration in mutant co-cultures infected with Ad-Rac1CA or Ad-Cdc42CA (data not shown). Mutant co-cultures infected with both Ad-Rac1CA and Ad-Cdc42CA showed slightly increased myelin formation when compared to untreated mutant co-cultures (compare Fig. 6F to 6E), but this increased myelination was not statistically significant (Fig. 6H,I). This result suggests that myelination might require additional signals induced by laminins. We cannot rule out the possibility that increasing Rac1 and/or Cdc42 activities could partially restore sorting and ensheathment defects in mutant co-cultures, because axons do not exist as bundles in the in vitro system making it difficult to analyze these effects.

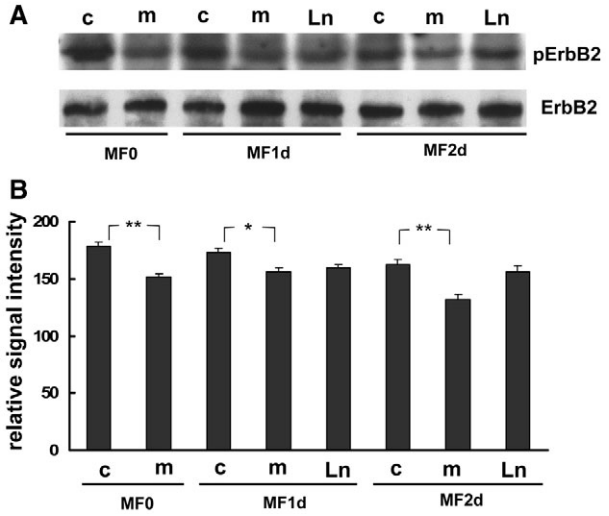

Fig. 5. SCs lacking laminins show decreased ErbB2 phosphorylation. (A) Phosphorylation of ErbB2 in control (c) and mutant (m) co-cultures before induction of myelination (MF0) and control (c), mutant (m), and mutant co-cultures with exogenous laminins (Ln) incubated for 1 or 2 days in MF (MF1d and MF2d, respectively) was assessed by immunoblot. (B) Quantitative analysis of phospho-ErbB2 normalized with total ErbB2 level in co-cultures at various time points. Triplicate assays; *P<0.05, **P<0.01; error bars, s.e.m. Phosphorylation of ErbB2 was decreased in co-cultures lacking laminins.

Forced activation of small GTPases improves sorting and hypomyelinating phenotypes of mutant nerves

To further address whether the sorting or the hypomyelinating defects in nerves lacking laminins can be improved by forced activation of Rac1 and/or Cdc42, we injected developing mutant nerves with Ad-Rac1CA and/or Ad-Cdc42CA at the common peroneal-tibialis bifurcation (arrow in Fig. 7A). Validation of the treatment was confirmed by eGFP expression in nerves infected with an adenovirus expressing eGFP, but not in nerves treated with saline (Fig. 7B,C). Contralateral nerves infected with control adenoviruses did not show significant improvement of mutant phenotypes, as many large unsorted bundles still existed (asterisks in Fig. 7D). By contrast, nerves treated with Rac1CA showed an improvement in sorting phenotype, as the average size of each unsorted bundle became significantly smaller after treatment (Fig. 7E,L). Nerves treated with Cdc42CA showed improvement as well. In this case, improvement was observed not only in sorting but also in myelinating phenotypes (Fig. 7F), as the average size of each bundle was smaller and the number of sorted myelinated fibers was increased when compared with nerves treated with control viruses (Fig. 7L,M). Sorting and myelination improvement was most evident when nerves were treated with both Rac1CA and Cdc42CA (Fig. 7G). Statistical analysis revealed that the average size of each bundle was significantly smaller and that the number of sorted myelinated fibers was significantly increased in nerves treated with Rac1CA and Cdc42CA (Fig. 7L,M). In nerves treated with both Rac1CA and Cdc42CA, some mutant SCs located near the unsorted axonal bundle reached a one-to-one relationship with an individual fiber (SC in Fig. 7I), but not in mutant nerves treated with control viruses (Fig. 7H), indicating that the sorting phenotype was improved after treatment. Many myelinated fibers surrounding the unsorted axonal bundles can also be observed in nerves treated with Rac1CA and Cdc42CA (arrows in Fig. 7K) but not in mutant nerves

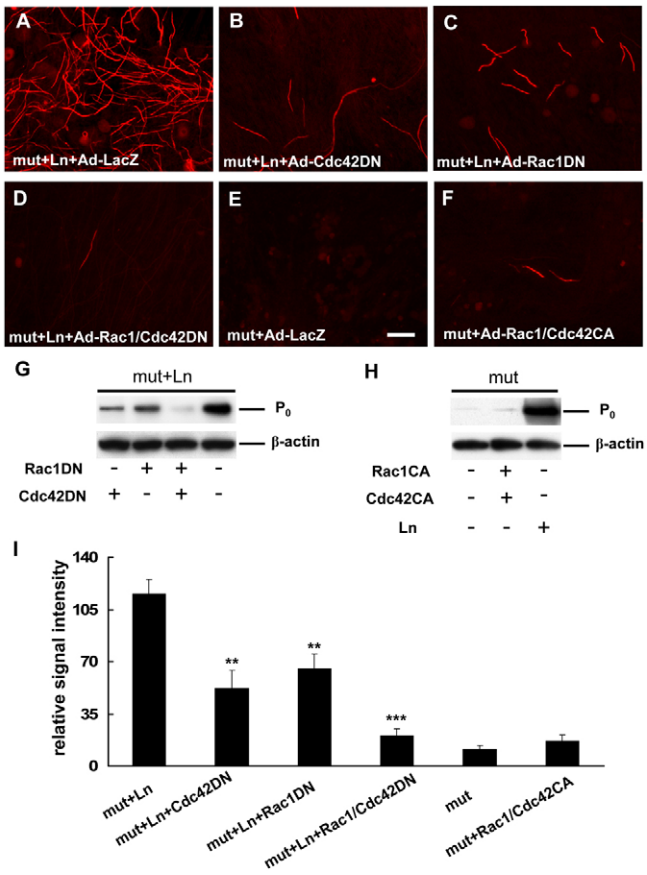

Fig. 6. Expression of Rac1DN and/or Cdc42DN in SCs attenuates laminin-induced myelination. Mutant co-cultures with exogenous laminins infected with Ad-LacZ (A), Ad-Cdc42DN (B), Ad-Rac1DN (C), or Ad-Rac1DN and Ad-Cdc42DN (D) at MF14 were stained for MBP to detect myelin formation. Mutant co-cultures infected with Ad-LacZ (E) or Ad-Rac1CA and Ad-Cdc42CA (F) at MF14 were stained for MBP to detect myelin formation. Scale bar: 50 μm. (G,H) The expression of P_0 in mutant co-cultures with (G) or without (H) exogenous laminins infected with various types of adenoviruses at MF14 was assessed by immunoblotting. β-Actin served as the loading control. (I) Quantitative analysis of immunoblot assay from (G) and (H). Signal intensity of P_0 was measured by ImageJ and normalized to β-actin. Triplicate assays; $^{**}P<0.01$, $^{***}P<0.001$ compared to signal intensity of mut+Ln. Myelination was decreased in mutant co-cultures treated with exogenous laminins that were infected with Ad-Cdc42DN and/or Ad-Rac1DN. Myelination was not significantly restored in mutant co-cultures infected with Ad-Rac1CA and Ad-Cdc42CA.

treated with control viruses (Fig. 7J), suggesting that these fibers could be newly sorted from the bundle and ensheathed with nascent myelin sheaths by mutant SCs after treatment. These results indicate that both Rac1 and Cdc42 are critical components of laminin downstream signals. Thus, laminin plays a pivotal role in coordinating both ErbB-Cdc42 and β1-integrin–Rac1 signaling pathways, which are essential for SC proliferation and process extension, respectively.

Discussion

SCs lacking β1 integrin or Rac1 show similar sorting phenotypes, where radial process extension is defective but SC proliferation is normal (Nodari et al., 2007). In contrast to β1-integrin-null or Rac1-null SCs, loss of Cdc42 in SCs results in decreased proliferation but does not affect process extension (Grove et al., 2007). Cdc42 is activated by NRG1 to promote SC proliferation during sorting. These results indicate that radial axonal sorting requires at least two parallel pathways: one stimulates SC proliferation, and the other promotes process extension. Previously, we showed that SCs lacking laminins have reduced proliferation, which probably resulted from decreased ErbB phosphorylation (Yu et al., 2005). In this report, our findings suggest that laminins are also required for process extension and regulate both Rac1 and Cdc42 activities (Fig. 4C).

Our results demonstrate that in addition to proliferation and process extension, laminins initiate SC bipolar shape formation. Laminins might regulate SC morphology through Schwannomin. The lack of Schwannomin in Schwannoma cells alters the characteristic bipolar shape of SCs, so that they are rounded in shape (Pelton et al., 1998; Rosenbaum et al., 1998). This phenotype is similar to SCs lacking laminins (Fig. 2E). Consistent with this observation, rat Schwannoma RT4 cells become spindle-like in shape when cultured with laminin-1 (Matsumura et al., 1997). As suggested by our results, laminins might trigger Schwannomin phosphorylation to initiate SC bipolar shape (Fig. 4A,B). In agreement with this, Schwannomin becomes rapidly phosphorylated on Ser518 by p21-activated kinase (Pak) when primary SCs are exposed to laminin-1 (Thaxton et al., 2007b).

SC morphology is also regulated by Schwannomin-mediated precise control of Rac1 activity (Nakai et al., 2006), as Schwannomin is a negative regulator of Rac1 and Pak (Shaw et al., 2001). In contrast to normal SCs that contain low Rac1 activity and elongate their processes along neurites, the Schwannoma cells show hyperactivation of Rac1 and fail to align their processes with neurites (Kaempchen et al., 2003; Nakai et al., 2006). Application of the Rac-specific inhibitor to Schwannoma restores the SC-axon interaction (Nakai et al., 2006). In a negative-feedback loop, Rac1 activates Pak to phosphorylate Schwannomin, which in turn prevents inhibition of Rac1 and/or Pak (Kissil et al., 2002; Xiao et al., 2002). Tight regulation of this signaling loop is essential for SC morphogenesis during differentiation. In SCs lacking laminins, both Rac1 activity and Schwannomin phosphorylation are decreased (Fig. 4), which might lead to deregulation of the signaling loop and cause impairment of SC morphogenesis during differentiation (Figs 2 and 3).

We observed that the hypomyelinating phenotype of mutant nerves was partially rescued after expression of both Rac1CA and Cdc42CA in nerves (Fig. 7G,K,M). However, this effect was not observed in mutant co-cultures with the same treatment (Fig. 6F,H,I). This difference could be attributed to the residual amount of laminin produced from perineural cells in mutant nerves (Yu et al., 2005). The expression of Rac1CA and Cdc42CA in SCs of mutant nerves resulted in more sorting of nerve bundles (Fig. 7L). These nerve fibers were then myelinated by mutant SCs that acquired laminins from nearby connective tissues (Fig. 7G,K). In mutant co-cultures, laminins were absent (Fig. 1B). Without any laminin, SCs in mutant co-cultures might not be able to myelinate axons even after forced activation of Rac1 and Cdc42. Therefore, molecules other than Rac1 and Cdc42 might be involved in promoting myelination downstream of laminins.

Axonal sorting is an essential step in the development of the peripheral nervous system, and laminin plays a critical role in this step (Yang et al., 2005; Yu et al., 2005). How laminin regulates axonal sorting is not completely understood. The work presented here provides strong evidence that laminins coordinate multiple signaling events for SC proliferation and morphogenesis during radial axonal sorting.

Journal of Cell Science

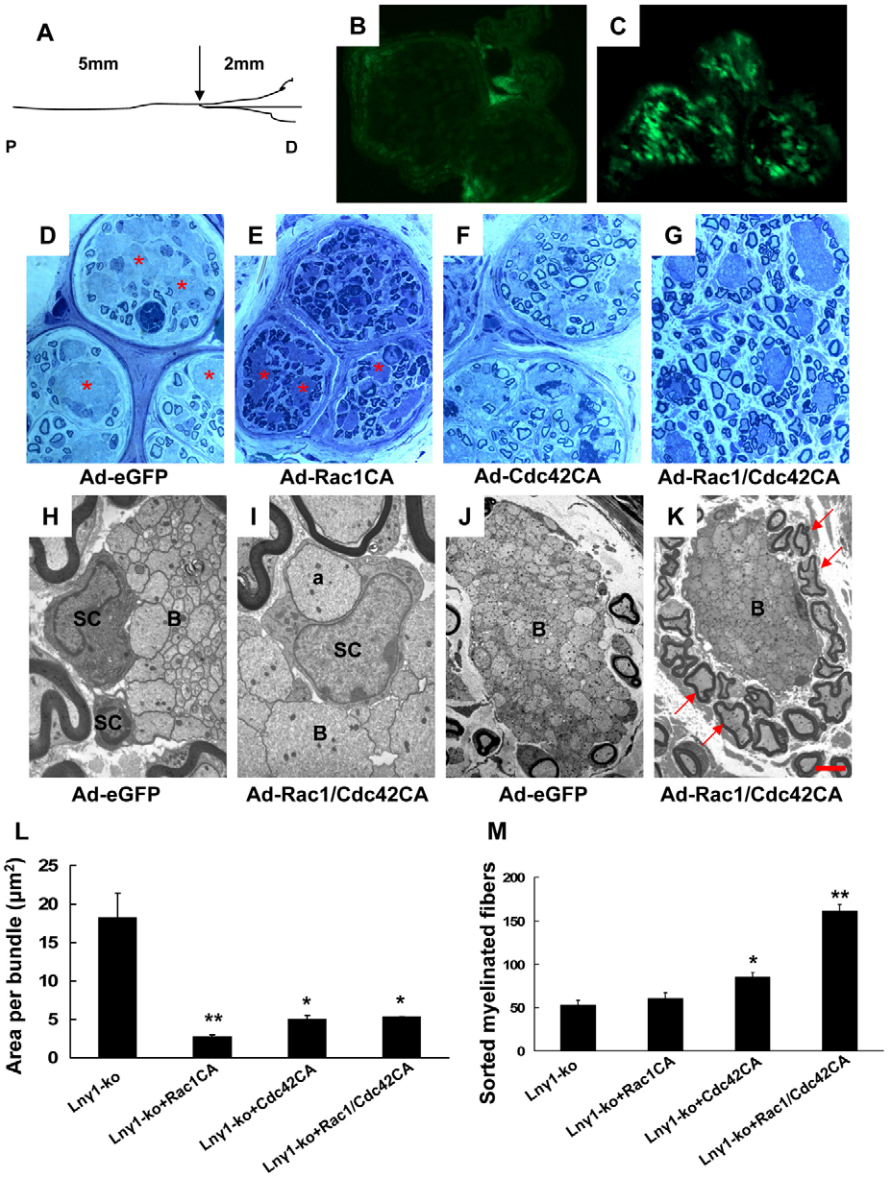

Fig. 7. The myelinating and sorting phenotypes of SCs lacking laminins are improved after treatment of an adenovirus expressing Rac1CA and/or Cdc42CA. Adenoviruses expressing eGFP, Rac1CA and/or Cdc42CA were injected into the endoneurium of P8 mutant sciatic nerve. Validation of the treatment was confirmed by eGFP expression (B and C). eGFP was expressed in nerves treated with Ad-eGFP (C) but not in nerves injected with saline (B). Two weeks after treatment (P22), transverse semithin (D-G) or ultrathin (H-K) sections were examined 1.5 mm proximal to the injection site. In mutant nerves treated with Ad-Rac1CA, the average size of each unsorted axonal bundle was reduced as compared with Ad-eGFP-treated nerves (asterisks, E vs D). In mutant nerves treated with Cdc42CA or with both viruses (Rac1CA and Cdc42CA), the average size of each unsorted axonal bundle was reduced and the total number of sorted myelinated fibers was increased as compared with Ad-eGFP-treated nerves (F and G vs D). Electron micrographs of nerves treated with both Rac1CA and Cdc42CA demonstrate that newly sorted (shown by 'a' in I) and myelinated fibers (arrows in K) were present when compared with Ad-eGFP-treated nerves (I and K vs H and J) (a, axon; B, unsorted bundle). Scale bar: 50 μm in B,C; 20 μm in D-G; 4 μm in H,I; 10 μm in J,K. (L) Statistical analysis revealed that the average area of each unsorted bundle significantly decreased in Rac1CA-treated nerves, Cdc42CA-treated nerves, and in nerves treated with Rac1CA and Cdc42CA (nine fields from three different animals in each group; $*P<0.05$, $**P<0.01$ by Student's *t*-test; error bars, s.e.m.). (M) Statistical analysis revealed that total sorted myelinated fibers significantly increased in Cdc42CA-treated nerves and in nerves treated with Rac1CA and Cdc42CA (nine fields from three different animals in each group; $*P<0.05$, $**P<0.01$ by Student's *t*-test; error bars, s.e.m.).

Materials and Methods

Mouse lines, immunocytochemistry, immunoblotting and electron microscopy

Mouse lines, immunocytochemistry, analysis of Cre-mediated *laminin γ1* gene recombination, immunoblotting and electron microscopy were described previously (Chen and Strickland, 2003; Yu et al., 2005). Antibodies used were rabbit anti-laminin-1 (Sigma), rat anti-MBP (Abcam, Cambridge, MA), rabbit anti-S100 (Swant, Bellinzona, Switzerland), rabbit anti-Schwannomin phospho-Ser518 (Rockland Immunochemicals, Gilbertsville, PA), rabbit anti-Schwannomin (Cell Signaling, Danvers, MA), rabbit anti-phospho-ErbB2 (Cell Signaling), rabbit anti-ErbB2 (Cell Signaling), and mouse anti-MPZ (gift from J. Archelos, Medical University Graz, Austria). All immunoblotting assays were in triplicate, and signal intensity of immunoblotting film was quantified by ImageJ software (NIH).

SC/DRG neuronal co-cultures

E14 mouse DRG were isolated, dissociated (Kleitman et al., 1999), plated onto 25 mm collagen-coated coverslips at a density of 25,000 cells per coverslip, and maintained in DMEM/F-12 (Invitrogen) containing 5% FBS with N2 supplement (Invitrogen) and 50 ng/ml nerve growth factor (NGF; Harlan, Indianapolis, IN). The endogenous SCs were allowed to proliferate and populate axons for 10 days. Co-cultures were infected with Ad-Cre (Microbix Biosystems, Toronto, Canada) or Ad-LacZ (Vector Biolabs, Philadelphia, PA) at a multiplicity of infection of 20 for another two days. Myelination was induced by the addition of fresh media containing 50 μg/ml ascorbate in the absence or presence of 25 μM exogenous mouse laminin-1 (Invitrogen). Adenoviruses expressing dominant negative Rac1 (Rac1DN), dominant negative Cdc42 (Cdc42DN), constitutively active Rac1 (Rac1CA), or constitutively active Cdc42 (Cdc42CA) (Cell Biolabs, San Diego, CA) were used to infect cells at a multiplicity of infection of 20 (or 10 each when two viruses were used in combination).

Rho GTPase assay

Activated Rac1 and Cdc42 were assessed by using a Rac1-Cdc42 activation assay kit (Chemicon) according to the manufacturer's instructions.

Generation of recombinant adenoviruses

cDNAs encoding eGFP-tagged β-actin (Clontech, Mountain View, CA) were subcloned into the *Sal*I and *Not*I sites of pShuttle-CMV (Stratagene, La Jolla, CA). The mCherry and mouse neurofilament light chain (NFL) cDNAs (Invitrogen) were inserted into the *Bgl*II, *Sal*I, and *Not*I sites of pShuttle-CMV, resulting in cDNAs encoding mCherry-tagged NFL. All constructs were verified by sequencing. Recombinant adenoviruses were produced using the AdEasy XL Adenoviral Vector System (Stratagene).

Time-lapse live-cell imaging

Cells were imaged using a Perkin-Elmer Ultraview spinning disk on a Zeiss Axiovert 200M microscope, using a 63×, 1.4 NA PlanApochromat objective, a Hamamatsu Orca ER cooled CCD camera, MetaMorph software for acquisition and analysis (Molecular Devices/MDS), and an environmental chamber (37°C, 5% CO_2; Solent Scientific). Stacks of 7-8 slices were acquired at 1 μm z-intervals at 5- or 15-minute

time intervals, imaging GFP (488 nm excitation, 500-550 nm emission) and mCherry (568 nm excitation, 590-650 nm emission) sequentially. For quantification of the axial axis (parallel to axons) to radial axis (vertical to axons) ratio of SCs, the axial axis and radial axis of eight control and mutant SCs from four fields of two independent assays were measured at 0, 3, 6, 9, 12 and 15 hours. For quantification of process extension rate and the length of processes, three independent videos (assays) for each group were analyzed for the first 12-hour periods. The number of newly formed processes was calculated each hour, and the length of process was measured when it reached the longest length (n=12-30 processes per assay).

Confocal microscopy of stained cells

Confocal microscopy was performed using a Zeiss LSM 510 Axiovert 200M microscope with 63×, 1.4 NA or 100×, 1.4 NA PlanApochromat objectives and a standard DAPI/FITC/Rhod/Cy5 Multitrack (405, 488, 543 and 633 nm laser lines). A pinhole diameter around 1 Airy unit was set for each channel to achieve equal optical slice thickness. Stacks of 35 z-sections were acquired at 0.2 μm z-intervals. Maximum projections were obtained using LSM Image Examiner software (Zeiss).

Adenovirus injection

Adenovirus injection was performed as described (Nodari et al., 2007). Adenovirus expressing eGFP (Ad-eGFP) was purchased from Cell Biolabs. P8 mice were anesthetized, and adenovirus (2 μl; 10^{11} viral particles/ml) was injected in the endoneurium of sciatic nerves at the common peroneal-tibialis bifurcation. One side of the nerve was injected with Ad-eGFP, and the other side was injected with Ad-Rac1CA and/or Ad-Cdc42CA. After two weeks, nerves were collected and processed for semithin and ultrathin sections as described previously (Chen and Strickland, 2003; Yu et al., 2005). For statistical analysis, the average area of each unsorted axonal bundle or the total number of sorted myelinated fibers present in each field of transverse semithin section 1.5 mm proximal to the injection site (three random fields from each animal; three animals in each group) was quantified by ImageJ software and analyzed using the Student's t-test.

We thank Laura Feltri for providing materials and helpful suggestions; Erin Norris for comments on the manuscript; and Prabhjot Dhadialla, Karen Carlson, Chia Chan and Huaxu Yu for useful discussions. This work was supported by grants from the NIH (NS038472), the Dr Miriam and Sheldon G. Adelson Medical Research Foundation, and the Muscular Dystrophy Association (MDA4066). Deposited in PMC for release after 12 months.

References

Benninger, Y., Thurnherr, T., Pereira, J. A., Krause, S., Wu, X., Chrostek-Grashoff, A., Herzog, D., Nave, K. A., Franklin, R. J., Meijer, D. et al. (2007). Essential and distinct roles for cdc42 and rac1 in the regulation of Schwann cell biology during peripheral nervous system development. *J. Cell Biol.* **177**, 1051-1061.

Chen, Z. L. and Strickland, S. (2003). Laminin gamma1 is critical for Schwann cell differentiation, axon myelination, and regeneration in the peripheral nerve. *J. Cell Biol.* **163**, 889-899.

Cosgaya, J. M., Chan, J. R. and Shooter, E. M. (2002). The neurotrophin receptor p75NTR as a positive modulator of myelination. *Science* **298**, 1245-1248.

Feltri, M. L., Graus Porta, D., Previtali, S. C., Nodari, A., Migliavacca, B., Cassetti, A., Littlewood-Evans, A., Reichardt, L. F., Messing, A., Quattrini, A. et al. (2002). Conditional disruption of beta 1 integrin in Schwann cells impedes interactions with axons. *J. Cell Biol.* **156**, 199-209.

Grove, M., Komiyama, N. H., Nave, K. A., Grant, S. G., Sherman, D. L. and Brophy, P. J. (2007). FAK is required for axonal sorting by Schwann cells. *J. Cell Biol.* **176**, 277-282.

Jessen, K. R. and Mirsky, R. (2005). The origin and development of glial cells in peripheral nerves. *Nat. Rev. Neurosci.* **6**, 671-682.

Kaempchen, K., Mielke, K., Utermark, T., Langmesser, S. and Hanemann, C. O. (2003). Upregulation of the Rac1/JNK signaling pathway in primary human schwannoma cells. *Hum. Mol. Genet.* **12**, 1211-1221.

Kissil, J. L., Johnson, K. C., Eckman, M. S. and Jacks, T. (2002). Merlin phosphorylation by p21-activated kinase 2 and effects of phosphorylation on merlin localization. *J. Biol. Chem.* **277**, 10394-10399.

Kleitman, N., Wood, P. M. and Bunge, R. P. (1999). Tissue culture methods for the study of myelination. In *Culturing Nerve Cells* (ed. G. Banker and K. Goslin), pp. 545-658. Cambridge: MIT Press.

Martin, J. R. and Webster, H. D. (1973). Mitotic Schwann cells in developing nerve: their changes in shape, fine structure, and axon relationships. *Dev. Biol.* **32**, 417-431.

Matsumura, K., Chiba, A., Yamada, H., Fukuta-Ohi, H., Fujita, S., Endo, T., Kobata, A., Anderson, L. V., Kanazawa, I., Campbell, K. P. et al. (1997). A role of dystroglycan in schwannoma cell adhesion to laminin. *J. Biol. Chem.* **272**, 13904-13910.

Morrissey, T. K., Levi, A. D., Nuijens, A., Sliwkowski, M. X. and Bunge, R. P. (1995). Axon-induced mitogenesis of human Schwann cells involves heregulin and p185erbB2. *Proc. Natl. Acad. Sci. USA* **92**, 1431-1435.

Nakai, Y., Zheng, Y., MacCollin, M. and Ratner, N. (2006). Temporal control of Rac in Schwann cell-axon interaction is disrupted in NF2-mutant schwannoma cells. *J. Neurosci.* **26**, 3390-3395.

Nobes, C. D. and Hall, A. (1995). Rho, rac, and cdc42 GTPases regulate the assembly of multimolecular focal complexes associated with actin stress fibers, lamellipodia, and filopodia. *Cell* **81**, 53-62.

Nodari, A., Zambroni, D., Quattrini, A., Court, F. A., D'Urso, A., Recchia, A., Tybulewicz, V. L., Wrabetz, L. and Feltri, M. L. (2007). Beta1 integrin activates Rac1 in Schwann cells to generate radial lamellae during axonal sorting and myelination. *J. Cell Biol.* **177**, 1063-1075.

Pelton, P. D., Sherman, L. S., Rizvi, T. A., Marchionni, M. A., Wood, P., Friedman, R. A. and Ratner, N. (1998). Ruffling membrane, stress fiber, cell spreading and proliferation abnormalities in human Schwannoma cells. *Oncogene* **17**, 2195-2209.

Riethmacher, D., Sonnenberg-Riethmacher, E., Brinkmann, V., Yamaai, T., Lewin, G. R. and Birchmeier, C. (1997). Severe neuropathies in mice with targeted mutations in the ErbB3 receptor. *Nature* **389**, 725-730.

Rosenbaum, C., Kluwe, L., Mautner, V. F., Friedrich, R. E., Muller, H. W. and Hanemann, C. O. (1998). Isolation and characterization of Schwann cells from neurofibromatosis type 2 patients. *Neurobiol. Dis.* **5**, 55-64.

Rouleau, G. A., Merel, P., Lutchman, M., Sanson, M., Zucman, J., Marineau, C., Hoang-Xuan, K., Demczuk, S., Desmaze, C., Plougastel, B. et al. (1993). Alteration in a new gene encoding a putative membrane-organizing protein causes neuro-fibromatosis type 2. *Nature* **363**, 515-521.

Salzer, J. L., Bunge, R. P. and Glaser, L. (1980). Studies of Schwann cell proliferation. III. Evidence for the surface localization of the neurite mitogen. *J. Cell Biol.* **84**, 767-778.

Shaw, R. J., Paez, J. G., Curto, M., Yaktine, A., Pruitt, W. M., Saotome, I., O'Bryan, J. P., Gupta, V., Ratner, N., Der, C. J. et al. (2001). The Nf2 tumor suppressor, merlin, functions in Rac-dependent signaling. *Dev. Cell* **1**, 63-72.

Thaxton, C., Lopera, J., Bott, M., Baldwin, M. E., Kalidas, P. and Fernandez-Valle, C. (2007a). Phosphorylation of the NF2 tumor suppressor in Schwann cells is mediated by Cdc42-Pak and requires paxillin binding. *Mol. Cell Neurosci.* **34**, 231-242.

Thaxton, C., Lopera, J., Bott, M. and Fernandez-Valle, C. (2007b). Neuregulin and laminin stimulate phosphorylation of the NF2 tumor suppressor in Schwann cells by distinct protein kinase A and p21-activated kinase-dependent pathways. *Oncogene*. **27**, 2705-2715.

Trofatter, J. A., MacCollin, M. M., Rutter, J. L., Murrell, J. R., Duyao, M. P., Parry, D. M., Eldridge, R., Kley, N., Menon, A. G., Pulaski, K. et al. (1993). A novel moesin-, ezrin-, radixin-like gene is a candidate for the neurofibromatosis 2 tumor suppressor. *Cell* **75**, 826.

Xiao, G. H., Beeser, A., Chernoff, J. and Testa, J. R. (2002). p21-activated kinase links Rac/Cdc42 signaling to merlin. *J. Biol. Chem.* **277**, 883-886.

Yang, D., Bierman, J., Tarumi, Y. S., Zhong, Y. P., Rangwala, R., Proctor, T. M., Miyagoe-Suzuki, Y., Takeda, S., Miner, J. H., Sherman, L. S. et al. (2005). Coordinate control of axon defasciculation and myelination by laminin-2 and -8. *J. Cell Biol.* **168**, 655-666.

Yu, W. M., Feltri, M. L., Wrabetz, L., Strickland, S. and Chen, Z. L. (2005). Schwann cell-specific ablation of laminin gamma1 causes apoptosis and prevents proliferation. *J. Neurosci.* **25**, 4463-4472.

Yu, W. M., Yu, H. and Chen, Z. L. (2007). Laminins in peripheral nerve development and muscular dystrophy. *Mol. Neurobiol.* **35**, 288-297.

Journal of Cell Science